

ARGONNE NATIONAL LABORATORY
9700 South Cass Avenue
Argonne, Illinois 60439

Convergence Analysis of Fixed Point Chance Constrained Optimal Power Flow Problems

J. J. Brust, M. Anitescu

Mathematics and Computer Science Division

Preprint ANL/MCS-P9431-0121

January 2021

arXiv:2101.11740v1 [math.OC] 27 Jan 2021

The submitted manuscript has been created by UChicago Argonne, LLC, Operator of Argonne National Laboratory (“Argonne”). Argonne, a U.S. Department of Energy Office of Science laboratory, is operated under Contract No. DE-AC02-06CH11357. The U.S. Government retains for itself, and others acting on its behalf, a paid-up nonexclusive, irrevocable worldwide license in said article to reproduce, prepare derivative works, distribute copies to the public, and perform publicly and display publicly, by or on behalf of the Government. The Department of Energy will provide public access to these results of federally sponsored research in accordance with the DOE Public Access Plan. <http://energy.gov/downloads/doe-public-accessplan>

Convergence Analysis of Fixed Point Chance Constrained Optimal Power Flow Problems

Johannes J. Brust, and Mihai Anitescu, *Member, IEEE*

Abstract—For optimal power flow problems with chance constraints, a particularly effective method is based on a fixed point iteration applied to a sequence of deterministic power flow problems. However, a priori, the convergence of such an approach is not necessarily guaranteed. This article analyses the convergence conditions for this fixed point approach, and reports numerical experiments including for large IEEE networks.

Index Terms—Fixed point method, Chance Constraints, Stochastic Optimizations, AC Optimal Power Flow

I. INTRODUCTION

CHANCE constrained optimization problems are typically computationally very challenging. However, when modeling the effects of uncertainty on optimal power networks, potentially large chance constrained optimization problems arise [1]–[5]. Commonly, stochastic optimal power flow models are developed by reformulating a widely accepted deterministic model. One such “classical” model is the AC optimal power flow model (AC-OPF) [6]. Because AC-OPF has multiple degrees of freedom with respect to the problem variables, various stochastic power flow paradigms can be developed from it. In particular, one can define different subsets of variables as stochastic variables. For instance, in [7] power generation is regarded as being stochastic (with constant demands), resulting in probabilistic objective functions. This article develops a chance constrained AC optimal power flow model (CC-AC-OPF) in which the objective function is deterministic, and the demands can be stochastic. This enables direct interpretation of the meaning of the optimal objective function values, and can be more realistic, given that in practice demand is far more a source of uncertainty as compared to supply. Yet, independent of how the stochastic power flow model is formulated it typically yields a chance constrained optimization problem. In order to also solve large instances of the resulting CC-AC-OPF problems, a fixed point iteration on a sequence of modified, related, and simpler deterministic AC-OPF problems is solved. Iterative methods that solve a sequence of simpler problems have been very effective on a variety of recent power systems problems [8]–[10]. In the context of chance-constrained optimization, such an approach has been successfully used in [11], [12] among more. However, prior to this work, there did not exist analytical criteria for when one can expect this fixed point iteration to converge. Therefore, this article describes a convergence analysis of the chance

constrained fixed point iteration and tests the method on a set of standard IEEE networks. The numerical experiments report results for networks with up to 9000 nodes. To summarize, the contributions of this work are: (1) The formulation of a new CC-AC-OPF model with a deterministic objective function, derived from uncertain demands; (2) The application and analysis of a fixed-point algorithm for an implicit chance constrained problem. Even though the use of iterative (fixed-point) techniques is widespread in power systems problems, previously no rigorous analysis had been undertaken for this formulation. In particular, we disentangle effects of model parameters and network properties on the convergence; (3) We include numerical experiments on large test cases.

A. AC Power Flow

The power network is defined by N nodes (buses) and N_L edges (lines). Associated to each bus is a voltage magnitude, v_i , frequency θ_i and a quantity that represents power generation or consumption at the i^{th} bus, for $1 \leq i \leq N$. In particular, let p_i^g be the real power generated at bus i , q_i^g the corresponding reactive power and p_i^d , q_i^d the real and reactive demands, respectively. The buses are furthermore divided into two groups: generators and loads. The indexing sets are G , and L , which are related to the set of all buses by $B = G \cup L$ and $N = N_G + N_L$. Throughout, we will use the indexing sets $\{G, L\}$ as subscripts to bold font vector variables. Note that in our setup each bus fits exactly into one of the two categories (though one can easily set a virtual zero load at a node). It is customary to assume that the network contains one reference bus (typically at $i = 1$). Load buses do not have active power generation and are thus defined by $\mathbf{p}_L^g = \mathbf{q}_L^g = \mathbf{0}$, where $\mathbf{p}^g, \mathbf{q}^g$ are vectors that contain the p_i^g 's and q_i^g 's. The power flow in the system is described by the power flow equations, which couple the variables (e.g., [6, Sections III-IV]). Specifically, let G_{ik}, B_{ik} denote the entries of the network's admittance matrix and define the quantities $\theta^{ik} \equiv \theta_i - \theta_k$, $c_{ik} \equiv G_{ik} \cos(\theta^{ik}) + B_{ik} \sin(\theta^{ik})$ and $d_{ik} \equiv G_{ik} \sin(\theta^{ik}) - B_{ik} \cos(\theta^{ik})$. With these definitions, the $2N$ power flow equations, for $i = 1, \dots, N$, are

$$\begin{aligned} v_i \sum_{k=1}^N v_k c_{ik} - (p_i^g - p_i^d) &= 0, \\ v_i \sum_{k=1}^N v_k d_{ik} - (q_i^g - q_i^d) &= 0, \end{aligned} \quad (1)$$

when grouped by busses. If we let $\mathbf{d} = \text{vec}(\mathbf{p}^d, \mathbf{q}^d)$ be the \mathbb{R}^{2N} vector containing p_i^d, q_i^d then in vector notation (1) is expressed as $\mathbf{f}(\mathbf{v}, \boldsymbol{\theta}, \mathbf{p}^g, \mathbf{q}^g; \mathbf{d}) = \mathbf{0}$, where \mathbf{f} represents the

J.J. Brust and M. Anitescu are with Argonne National Laboratory, Mathematics and Computer Science Division, Lemont, IL, e-mails: jbrust@anl.gov, anitescu@mcsl.anl.gov

This work was supported by the U.S. Department of Energy, Office of Science, Advanced Scientific Computing Research, under Contract DE-AC02-06CH11357 at Argonne National Laboratory.

nonlinear equations in (1). Note, however, that \mathbf{f} is linear in \mathbf{d} , a fact we will use later. Moreover, \mathbf{d} is regarded as a parameter and not a variable.

B. AC Optimal Power Flow

Optimal power flow determines the best set of variables that satisfy the network constraints. In addition to the power flow equations from (1), branch current bounds are typically included in the optimization problem. In particular, let LC be the set of all line connections, i.e., the set of index pairs that describe all line connections. For instance, if bus i is connected to bus k , then $(i, k) \in LC$. Subsequently, the so-called branch current constraints are $(D_{ik}^{\max})^2 - (v_i \cos(\theta_i) - v_k \cos(\theta_k))^2 - (v_i \sin(\theta_i) - v_k \sin(\theta_k))^2 \geq 0$, $\forall (i, k) \in LC$ for constant current limits D_{ik}^{\max} . In vector notation these N_L constraints are represented as $\mathbf{g}(\mathbf{v}, \boldsymbol{\theta}) \geq \mathbf{0}$. It is also desirable to include ‘‘hard’’ bounds on the generation variables, such as $\mathbf{l}_p \leq \mathbf{p}_G^g \leq \mathbf{u}_p$, where \mathbf{l}_p , \mathbf{u}_p represent constant lower and upper bounds. The AC optimal power flow (AC-OPF) problem, for a cost function C_0 , is thus formulated as

$$\underset{\mathbf{v}, \boldsymbol{\theta}, \mathbf{p}^g, \mathbf{q}^g}{\text{minimize}} C_0(\mathbf{p}_G^g) \quad \text{subject to} \quad (2)$$

$$\mathbf{f}(\mathbf{v}, \boldsymbol{\theta}, \mathbf{p}^g, \mathbf{q}^g; \mathbf{d}) = \mathbf{0} \quad (3)$$

$$\mathbf{g}(\mathbf{v}, \boldsymbol{\theta}) \geq \mathbf{0}$$

$$\mathbf{l}_p \leq \mathbf{p}_G^g \leq \mathbf{u}_p$$

$$\mathbf{l}_q \leq \mathbf{q}_G^g \leq \mathbf{u}_q$$

$$\mathbf{l}_v \leq \mathbf{v} \leq \mathbf{u}_v$$

$$\mathbf{l}_\theta \leq \boldsymbol{\theta} \leq \mathbf{u}_\theta$$

The cost function is typically a convex quadratic function that only depends on the real power generation. Specifically, $C_0(\mathbf{p}_G^g) = \sum_{i \in G} q_{ii} (p_i^g)^2 + \sum_{i \in G} q_i p_i^g + q_{00}$ for cost data q_{ii} , q_i and q_{00} . The solution $\mathbf{s}^* = \text{vec}(\mathbf{v}^*, \boldsymbol{\theta}^*, (\mathbf{p}^g)^*, (\mathbf{q}^g)^*)$ of (2) is called the optimal power flow point, or OPF point.

C. Chance Constrained AC Optimal Power Flow

In order to introduce uncertainty related to e.g., renewable energy into the OPF problem (2) we regard the demand terms in (1) (i.e., p_i^d, q_i^d) as forecasted values with possible error. Specifically, these stochastic quantities are represented as

$$p_i^d + \omega_i, \quad q_i^d + \omega_{N+i}, \quad (4)$$

where ω_i and ω_{N+i} represent forecasting errors. For compactness, the stochastic errors are represented by the $2N$ vector $\boldsymbol{\omega}$. Here we assume $\boldsymbol{\omega}$ is normal, and relaxing this assumption yields different approaches. The chance constrained AC-OPF model in this Section is developed such that the objective function only depends on deterministic variables. When the objective function represents cost, deterministic values are meaningful and important. Since the power flow equations in (1) are overdetermined, i.e., $\mathbf{f} : \mathbb{R}^{2N+N_G} \rightarrow \mathbb{R}^{2N}$, this system has N_G degrees of freedom. Subsequently, let $\mathbf{y} = \mathbf{p}_G$ represent a \mathbb{R}^{N_G} vector of deterministic variables and $\mathbf{x} = \mathbf{x}(\boldsymbol{\omega}) = \text{vec}(\mathbf{q}_G(\boldsymbol{\omega}), \mathbf{v}_L(\boldsymbol{\omega}), \boldsymbol{\theta}(\boldsymbol{\omega}))$ a $2N$ vector of

stochastic variables. The stochastic power flow equations are represented as

$$\mathbf{f}(\mathbf{x}, \mathbf{y}; \mathbf{d}) + \boldsymbol{\omega} = \mathbf{f}_\omega(\mathbf{x}(\boldsymbol{\omega}), \mathbf{y}; \mathbf{d} + \boldsymbol{\omega}) \equiv \mathbf{f}_\omega = \mathbf{0}. \quad (5)$$

If $\boldsymbol{\omega} = \mathbf{0}$ these equations reduce to the power flow equations in (1). Note that the power flow equations couple the variables and that the uncertainty in \mathbf{x} depends on the uncertainty in the demands ‘‘ \mathbf{d} ’’, since $\mathbf{x} = \mathbf{x}(\boldsymbol{\omega}) = \mathbf{x}(\mathbf{y}, \mathbf{d} + \boldsymbol{\omega})$. We set $C_0(\mathbf{p}_G^g) = C_0(\mathbf{y})$ to reflect the change in variables for the stochastic optimal power flow problem and note that the objective function is deterministic. Let $\mathbb{P}(\mathbf{z} \geq \mathbf{0}) \geq 1 - \epsilon$ represent a vector of inequalities with non-negative probability constraints, for which each element in the left hand side corresponds to a cumulative probability (for $z_i \geq 0$) and each element of ϵ is in the interval $0 < \epsilon < 1$. Then the chance constrained (stochastic) optimal power flow problem is given by

$$\underset{\mathbf{x}(\boldsymbol{\omega}), \mathbf{y}}{\text{minimize}} C_0(\mathbf{y}) \quad \text{subject to} \quad (6)$$

$$\mathbf{f}_\omega(\mathbf{x}(\boldsymbol{\omega}), \mathbf{y}; \mathbf{d} + \boldsymbol{\omega}) = \mathbf{0} \quad \forall \boldsymbol{\omega}$$

$$\mathbb{P}(\mathbf{g}(\mathbf{x}(\boldsymbol{\omega}), \mathbf{y}) \geq \mathbf{0}) \geq \mathbf{1} - \epsilon_g \quad (7)$$

$$\mathbb{P}(\mathbf{l}_x \leq \mathbf{x}(\boldsymbol{\omega}) \leq \mathbf{u}_x) \geq \mathbf{1} - \epsilon_x \quad (8)$$

$$\mathbf{l}_y \leq \mathbf{y} \leq \mathbf{u}_y.$$

Observe that the problem in (6) includes chance constraints (probability constraints) on the line flow limits (7) and the stochastic variables $\mathbf{x}(\boldsymbol{\omega})$ (8), while deterministic limits are set on \mathbf{y} . Here ϵ_g and ϵ_x correspond to model parameters for setting probability thresholds.

1) *Computing Chance Constraints:* To practically compute the chance constraints in problem (6), the stochastic variables are linearized around the error $\boldsymbol{\omega}$ (zero mean), similar to [11]. This is equivalent to assuming that $\boldsymbol{\omega}$ is sufficiently small, which we proceed to do in the rest of the paper. In particular,

$$\mathbf{x}(\mathbf{y}, \mathbf{d} + \boldsymbol{\omega}) \approx \mathbf{x}(\mathbf{y}, \mathbf{d}) + \left. \frac{\partial \mathbf{x}(\mathbf{y}, \mathbf{d} + \boldsymbol{\omega})}{\partial \boldsymbol{\omega}} \right|_{\boldsymbol{\omega}=\mathbf{0}} \boldsymbol{\omega} \equiv \mathbf{x}_\omega. \quad (9)$$

Note that $\mathbf{x}(\mathbf{y}, \mathbf{d}) = \mathbf{x}_0$ and that $\partial \mathbf{x}(\mathbf{y}, \mathbf{d}) / \partial \boldsymbol{\omega}$ are deterministic. Thus the expectation and variance of \mathbf{x}_ω are $\mathbb{E}[\mathbf{x}_\omega] = \mathbf{x}(\mathbf{y}, \mathbf{d}) = \mathbf{x}_0$, and $\text{Var}[\mathbf{x}_\omega] = (\partial \mathbf{x}(\mathbf{y}, \mathbf{d}) / \partial \boldsymbol{\omega}) \text{Var}[\boldsymbol{\omega}] (\partial \mathbf{x}(\mathbf{y}, \mathbf{d}) / \partial \boldsymbol{\omega})^\top$, respectively. Because computing the full nonlinear probability constraints is typically very computationally expensive, the probabilities of the linearized random variables are used instead. For instance, the constraints from (8) are written as

$$\mathbb{P}(\mathbf{x}_\omega \leq \mathbf{u}_x) \geq \mathbf{1} - \epsilon_x, \quad \mathbb{P}(\mathbf{l}_x \leq \mathbf{x}_\omega) \geq \mathbf{1} - \epsilon_x. \quad (10)$$

To handle the vector of probabilities in (10) one can use a Bonferroni bound [13], in which each individual variable $(\mathbf{x}_\omega)_r$ for $1 \leq r \leq 2N$ satisfies an individual highly conservative probability constraint. However, when the variables are independent (or can be treated as such) then the probabilities can be separated without restrictions. The mean of $(\mathbf{x}_\omega)_r$ is $(\mathbf{x}_0)_r$, while the variance can also be explicitly computed. Define

$$\partial \mathbf{x} / \partial \boldsymbol{\omega} \equiv \boldsymbol{\Gamma}, \quad (11)$$

and let \mathbf{e}_r be the r^{th} column of the identity matrix. Moreover, denote $\text{Var}[\boldsymbol{\omega}] = \boldsymbol{\Sigma}^2$. With this the variance of $(\mathbf{x}_\omega)_r$ is $\|\mathbf{e}_r^\top \boldsymbol{\Gamma} \boldsymbol{\Sigma}\|_2^2$. In turn, when the variables can be treated independently, individual probability constraints, such as $F^{\text{Nrm}}((\mathbf{x}_\omega)_r \leq (\mathbf{u}_x)_r) \geq 1 - (\boldsymbol{\epsilon}_x)_r$ (where F^{Nrm} is the normal distribution function) can be represented as

$$((\mathbf{u}_x)_r - (\mathbf{x}_\omega)_r) / \|\mathbf{e}_r^\top \boldsymbol{\Gamma} \boldsymbol{\Sigma}\|_2 \geq (F^{\text{Nrm}})^{-1}(1 - (\boldsymbol{\epsilon}_x)_r),$$

where $(F^{\text{Nrm}})^{-1}(\cdot)$ is the inverse cumulative distribution function. Defining $z_r = (F^{\text{Nrm}})^{-1}(1 - (\boldsymbol{\epsilon}_x)_r)$ the constraints are represented as

$$(\mathbf{u}_x)_r - \lambda_r \geq (\mathbf{x}_\omega)_r, \quad \lambda_r = z_r \|\mathbf{e}_r^\top \boldsymbol{\Gamma} \boldsymbol{\Sigma}\|_2. \quad (12)$$

Similarly, for $2N + 1 \leq r_1 \leq 2N + N_L$ and $\bar{r}_1 = r_1 - 2N$, defining $z_{r_1} = (F^{\text{Nrm}})^{-1}(1 - (\boldsymbol{\epsilon}_g)_{r_1})$ the remaining probability constraints are represented as $\mathbf{g}(\mathbf{x}_0, \mathbf{y})_{\bar{r}_1} - \lambda_{r_1} \geq \mathbf{0}$ with

$$\lambda_{r_1} = z_{r_1} \|\mathbf{e}_{\bar{r}_1}^\top (\partial \mathbf{g} / \partial \mathbf{x}) \boldsymbol{\Gamma} \boldsymbol{\Sigma}\|_2. \quad (13)$$

Note that λ_r, λ_{r_1} depend on \mathbf{x}, \mathbf{y} and \mathbf{d} , e.g., $\lambda_r = \lambda_r(\mathbf{x}(\mathbf{y}, \mathbf{d}))$, which we will use later. Moreover the inequality in (12) is deterministic and thus straightforward to compute once $\boldsymbol{\Gamma}$ is known. Second, when $(\boldsymbol{\epsilon}_x)_r$ is a small number (which is typically the case) then $z_r > 0$ and $\lambda_r > 0$. Thus the λ_r, λ_{r_1} values are regarded as constraint tightenings and represent the effects of stochasticity in the constraints.

2) *Computing $\partial \mathbf{x} / \partial \boldsymbol{\omega}$* : The partial derivatives $\partial \mathbf{x} / \partial \boldsymbol{\omega} = \boldsymbol{\Gamma}$ in (12) are obtained by using the power flow equation

$$\frac{\partial}{\partial \boldsymbol{\omega}} (\mathbf{f}_\omega(\mathbf{x}(\boldsymbol{\omega}), \mathbf{y}; \mathbf{d} + \boldsymbol{\omega})) = \frac{\partial \mathbf{f}_\omega}{\partial \mathbf{x}} \frac{\partial \mathbf{x}}{\partial \boldsymbol{\omega}} + \frac{\partial \mathbf{f}_\omega}{\partial \boldsymbol{\omega}} = \mathbf{0}.$$

First, note from (5) that $\partial \mathbf{f}_\omega / \partial \boldsymbol{\omega} = \mathbf{I}$. Second, the partial derivatives are only needed at $\boldsymbol{\omega} = \mathbf{0}$, which yields the representation $\partial \mathbf{x} / \partial \boldsymbol{\omega} = -(\partial \mathbf{f}_0 / \partial \mathbf{x})^{-1}$ with the convention $\mathbf{f}_0 = \mathbf{f}$. Since $\mathbf{x} = \text{vec}(\mathbf{q}_G^g, \mathbf{v}_L, \boldsymbol{\theta})$ the so-called Jacobian matrix of partial derivatives is given by

$$\frac{\partial \mathbf{f}}{\partial \mathbf{x}} = \begin{bmatrix} \frac{\partial \mathbf{f}}{\partial \mathbf{q}_G^g} & \frac{\partial \mathbf{f}}{\partial \mathbf{v}_L} & \frac{\partial \mathbf{f}}{\partial \boldsymbol{\theta}} \end{bmatrix}. \quad (14)$$

The elements of this matrix can be computed from (1). Note that only the last N equations in (1) depend on \mathbf{q}^g . Subsequently, we define the indices $1 \leq i \leq N$ and $j = N + i$, as well as $1 \leq g \leq N_G$, $1 \leq l \leq N_L$ and $1 \leq t \leq N$. With this, the elements of the Jacobian from (14) are:

$$\begin{aligned} \left(\frac{\partial \mathbf{f}}{\partial \mathbf{q}_G^g} \right)_{i,g} &= 0, \\ \left(\frac{\partial \mathbf{f}}{\partial \mathbf{q}_G^g} \right)_{j,g} &= \begin{cases} -1 & \text{if } i = [G]_g \\ 0 & \text{otherwise} \end{cases} \\ \left(\frac{\partial \mathbf{f}}{\partial \mathbf{v}_L} \right)_{i,l} &= \begin{cases} \sum_{k=1}^N v_k c_{ik} + 2c_{ii} v_i & \text{if } i = [L]_l \\ v_i c_{i[L]_l} & \text{otherwise} \end{cases} \\ \left(\frac{\partial \mathbf{f}}{\partial \mathbf{v}_L} \right)_{j,l} &= \begin{cases} \sum_{k=1}^N v_k d_{ik} + 2d_{ii} v_i & \text{if } i = [L]_l \\ v_i d_{i[L]_l} & \text{otherwise} \end{cases} \\ \left(\frac{\partial \mathbf{f}}{\partial \boldsymbol{\theta}} \right)_{i,t} &= \begin{cases} -v_i \sum_{k=1}^N v_k d_{ik} & \text{if } i = t \\ v_i v_t d_{it} & \text{otherwise} \end{cases} \\ \left(\frac{\partial \mathbf{f}}{\partial \boldsymbol{\theta}} \right)_{j,t} &= \begin{cases} v_i \sum_{k=1}^N v_k c_{ik} & \text{if } i = t \\ -v_i v_t c_{it} & \text{otherwise} \end{cases} \end{aligned} \quad (15)$$

The partial derivatives $\partial \mathbf{x} / \partial \boldsymbol{\omega} = (\partial \mathbf{f} / \partial \mathbf{x})^{-1}$ are defined by an inverse. This inverse is typically well defined for regular optimal power flow problems, as described in [7, Section III. B] and [14]. Therefore, the smallest singular value of $\partial \mathbf{f} / \partial \mathbf{x} \equiv \mathbf{J}$ is positive, i.e., $\sigma_{\min}(\mathbf{J}) > 0$. A positive lower bound for the smallest singular value of a matrix is described in [15, Theorem 1]. Let $\mathbf{J}_{:,i}$ denote the i^{th} column of \mathbf{J} and let $\mathbf{J}_{i,:}$ be the i^{th} row of \mathbf{J} . Then a lower bound for the smallest singular value is:

$$\sigma_{\min}(\mathbf{J}) \geq \hat{K}_\Gamma > 0,$$

where

$$\hat{K}_\Gamma = \left(\frac{\hat{n} - 1}{\hat{n}} \right)^{\frac{\hat{n}-1}{2}} |\mathbf{J}| \max \left(\frac{\min(\|\mathbf{J}_{:,i}\|_2)}{\prod_i \|\mathbf{J}_{:,i}\|_2}, \frac{\min(\|\mathbf{J}_{i,:}\|_2)}{\prod_i \|\mathbf{J}_{i,:}\|_2} \right),$$

$\hat{n} \equiv 2N$, and where the determinant is $|\mathbf{J}| = \det(\mathbf{J})$. This means that

$$\|(\partial \mathbf{f} / \partial \mathbf{x})^{-1}\|_2 = \|\mathbf{J}^{-1}\|_2 = \frac{1}{\sigma_{\min}(\mathbf{J})} \leq 1 / \hat{K}_\Gamma \equiv K_\Gamma \quad (16)$$

where \hat{K}_Γ, K_Γ are finite constants. In order to compute solves with \mathbf{J} (which is part of computing the constraints in (12) and (13)) the LU factorization is based on the decomposition $\mathbf{J} = \mathbf{P}\mathbf{L}\mathbf{U}$, where \mathbf{P} is a permutation matrix, \mathbf{L} is a unit lower triangular matrix and \mathbf{U} is an upper triangular matrix. The determinant and the bounds in (16) are thus available “without extra expense” based on solves with \mathbf{J} , by multiplying the diagonal elements of \mathbf{U} , since $|\mathbf{J}| = |\mathbf{U}|$ and \mathbf{U} is upper triangular.

D. Implicit Chance Constrained Optimal Power Flow

An optimal power flow problem that combines components of the AC-OPF problem in (2) and of the chance constrained problem in (6) is obtained by using the constraints from (12) and (13). This reformulated problem incorporates stochastic effects, while at the same time enables efficient computations. The corresponding *implicit* chance-constrained AC-OPF problem is:

$$\begin{aligned} & \underset{\mathbf{v}, \boldsymbol{\theta}, \mathbf{p}^g, \mathbf{q}^g}{\text{minimize}} \quad C_0(\mathbf{p}_G^g) \quad \text{subject to} \\ & \mathbf{f}(\mathbf{v}, \boldsymbol{\theta}, \mathbf{p}^g, \mathbf{q}^g; \mathbf{d}) = \mathbf{0} \\ & \mathbf{g}(\mathbf{v}, \boldsymbol{\theta}) \geq \boldsymbol{\lambda}_g(\mathbf{p}_G^g) \\ & \mathbf{l}_q + \boldsymbol{\lambda}_q(\mathbf{p}_G^g) \leq \mathbf{q}_G^g \leq \mathbf{u}_q - \boldsymbol{\lambda}_q(\mathbf{p}_G^g) \\ & \mathbf{l}_v + \boldsymbol{\lambda}_v(\mathbf{p}_G^g) \leq \mathbf{v}_L \leq \mathbf{u}_v - \boldsymbol{\lambda}_v(\mathbf{p}_G^g) \\ & \mathbf{l}_\theta + \boldsymbol{\lambda}_\theta(\mathbf{p}_G^g) \leq \boldsymbol{\theta} \leq \mathbf{u}_\theta - \boldsymbol{\lambda}_\theta(\mathbf{p}_G^g) \\ & \mathbf{l}_p \leq \mathbf{p}_G^g \leq \mathbf{u}_p, \end{aligned} \quad (17)$$

where $\boldsymbol{\lambda}_q(\mathbf{p}_G^g), \boldsymbol{\lambda}_v(\mathbf{p}_G^g), \boldsymbol{\lambda}_\theta(\mathbf{p}_G^g)$ are computed using (12) and $\boldsymbol{\lambda}_g(\mathbf{p}_G^g)$ is computed using (13). The problem can be seen to be implicit with regards to probability constraints, because the effects of uncertainty are implicitly included in the tightenings of some constraints by the non-negative $\boldsymbol{\lambda}$'s.

II. METHOD

The solution of the potentially large nonlinear optimization problem in (17) can be computed directly. However, the computation of the λ 's adds nonlinearities, because they depend on the matrix $\Gamma = -(\partial \mathbf{x} / \partial \boldsymbol{\omega})^{-1} \in \mathbb{R}^{2N \times 2N}$, which is an inverse. Because of this, the problem in (17) is still computationally difficult. Instead of solving (17) directly, we describe an iterative scheme, which computes an approximate solution of (17), by solving a sequence of simpler problems (see also [11]). The algorithm is stated as:

Algorithm 1

- 1: Inputs: $\mathbf{s}^{(0)} = \text{vec}(\mathbf{v}^{(0)}, \boldsymbol{\theta}^{(0)}, \mathbf{p}^{(0)}, \mathbf{q}^{(0)})$, $0 < \tau_q$, $0 < \tau_v$, $0 < \tau_\theta$, $0 < \tau_g$, $0 < \epsilon_q \leq 0.5$, $0 < \epsilon_v \leq 0.5$, $0 < \epsilon_\theta \leq 0.5$, $0 < \epsilon_g \leq 0.5$, $0 < \Sigma$, $\lambda_q^{(0)} = \lambda_v^{(0)} = \lambda_\theta^{(0)} = \lambda_g^{(0)} = 0$, $k = 0$;
- 2: for $k = 0, 1, \dots$
- 3: Solve (17) with $\lambda_q^{(k)}, \lambda_v^{(k)}, \lambda_\theta^{(k)}$ fixed and obtain $\mathbf{s}^{(k+1)}$;
- 4: Compute $\lambda_q^{(k+1)}, \lambda_v^{(k+1)}, \lambda_\theta^{(k+1)}, \lambda_g^{(k+1)}$ using (12) and (13);
- 5: **if**

$$\begin{aligned} \|\lambda_q^{(k+1)} - \lambda_q^{(k)}\|_\infty &\leq \tau_q \text{ and} \\ \|\lambda_v^{(k+1)} - \lambda_v^{(k)}\|_\infty &\leq \tau_v \text{ and} \\ \|\lambda_\theta^{(k+1)} - \lambda_\theta^{(k)}\|_\infty &\leq \tau_\theta \text{ and} \\ \|\lambda_g^{(k+1)} - \lambda_g^{(k)}\|_\infty &\leq \tau_g \end{aligned}$$
then
 - 6: Stop. Return $\mathbf{s}^{(k+1)}$;
 - 7: **else**
 - 8: $k = k + 1$;
 - 9: **end if**

Note that Algorithm 1 stops when the changes in the λ 's become small. However no criteria have yet been specified for when one can expect the iteration to converge. Therefore, we analyze conditions for which one can expect Algorithm 1 to converge.

III. ANALYSIS

The analysis of Algorithm 1 is based on the observation that this iterative algorithm is a fixed point iteration. Therefore, in order to derive its convergence conditions, we investigate the convergence conditions of the fixed point iteration. Throughout this section, the problem from (17) is reformulated as

$$\begin{aligned} &\underset{\mathbf{s}}{\text{minimize}} C_1(\mathbf{s}) \quad \text{subject to} & (18) \\ &\mathbf{f}(\mathbf{s}) = \mathbf{0}, \quad \mathbf{h}(\mathbf{s}; \boldsymbol{\lambda}) \geq \mathbf{0} \end{aligned}$$

with $\mathbf{s} = \text{vec}(\mathbf{v}, \boldsymbol{\theta}, \mathbf{p}^g, \mathbf{q}^g)$, $C_1(\mathbf{s}) = C_0(\mathbf{p}_G^g)$, $\boldsymbol{\lambda} = \boldsymbol{\lambda}(\mathbf{s}) = \text{vec}(\lambda_q, \lambda_v, \lambda_\theta, \lambda_g)$, $\mathbf{h}(\mathbf{s}; \boldsymbol{\lambda}) \geq \mathbf{0} \in \mathbb{R}^m$ ($m = N_L + 4N$ inequality constraints in (17) parametrized by $\boldsymbol{\lambda}$) and $\mathbf{f}(\mathbf{s}; \mathbf{d}) = \mathbf{f}(\mathbf{s})$. Our analysis is consistent with classical nonlinear programming sensitivity results [16], [17], however is different because of the fixed point component of the algorithm. In classical nonlinear programming $\boldsymbol{\lambda}$ is taken as an independent perturbation parameter, with focus on the sensitivities of \mathbf{s}

with respect to $\boldsymbol{\lambda}$. However, because the (implicit) chance-constrained problem also contains the dependence $\boldsymbol{\lambda} = \boldsymbol{\lambda}(\mathbf{s})$ we are led to also acknowledge the interplay of $\boldsymbol{\lambda}$ and \mathbf{s} . Recall that a fixed point, say $\boldsymbol{\lambda}^*$, of the function, say $h(\boldsymbol{\lambda})$, is defined by the two conditions

$$\begin{aligned} h(\boldsymbol{\lambda}^*) &= \boldsymbol{\lambda}^*, & \|\partial h(\boldsymbol{\lambda}^*) / \partial \boldsymbol{\lambda}\|_2 &\in [0, 1], \end{aligned} \quad (19)$$

Condition 1 Condition 2

cf. [18]. To investigate the relation between the variables in Algorithm 1, define the mapping in line 3 that determines $\mathbf{s}^{(k+1)}$ from $\boldsymbol{\lambda}^{(k)}$ by $s_M(\boldsymbol{\lambda}^{(k)})$ (i.e., $\mathbf{s}^{(k+1)} = s_M(\boldsymbol{\lambda}^{(k)})$), and the operation in line 4 that determines $\boldsymbol{\lambda}^{(k+1)}$ from $\mathbf{s}^{(k+1)}$ by $\lambda_M(\mathbf{s}^{(k+1)})$ (i.e., $\boldsymbol{\lambda}^{(k+1)} = \lambda_M(\mathbf{s}^{(k+1)})$). Then the statements in the algorithm recursively define the next iterates, starting from $k = 0$, $\mathbf{s}^{(k)}$, $\boldsymbol{\lambda}^{(k)}$, so that,

$$\begin{aligned} \mathbf{s}^{(k+1)} &= s_M(\boldsymbol{\lambda}^{(k)}), & \boldsymbol{\lambda}^{(k+1)} &= \lambda_M(\mathbf{s}^{(k+1)}) \\ &= s_M(\lambda_M(\mathbf{s}^{(k)})), & &= \lambda_M(s_M(\boldsymbol{\lambda}^{(k)})). \end{aligned}$$

This means that there is a mapping that generates $\mathbf{s}^{(k+1)}$ from $\mathbf{s}^{(k)}$ and one that generates $\boldsymbol{\lambda}^{(k+1)}$ from $\boldsymbol{\lambda}^{(k)}$. In particular, if $\boldsymbol{\lambda}^{(k)} \rightarrow \boldsymbol{\lambda}^*$ then $\mathbf{s}^{(k)} \rightarrow \mathbf{s}^*$ and vice-versa. In the remainder of this section let the fixed points be denoted as $\boldsymbol{\lambda} = \boldsymbol{\lambda}^*$ and $\mathbf{s} = \mathbf{s}^*$. Our analysis is based on the assertion that if $\boldsymbol{\lambda}$ (and \mathbf{s}) is a fixed point, then Condition 2 in (19) holds. In particular, we analyze the expression

$$(\lambda_M(\mathbf{s}(\boldsymbol{\lambda})))_r = z_r \|\mathbf{e}_r^\top \Gamma(\mathbf{s}(\boldsymbol{\lambda})) \Sigma\|_2,$$

which is (12) with explicit dependencies on \mathbf{s} and $\boldsymbol{\lambda}$. (The conditions for (13) are done in a similar way, with an additional constant for the derivatives of the line flow constraints: $\|\partial \mathbf{g} / \partial \mathbf{x}\|_2 \leq K_g$). The solution to the nonlinear programming problem (18) is characterized by a set of optimality conditions. These conditions are defined by the Lagrangian:

$$L(\mathbf{s}, \boldsymbol{\mu}, \boldsymbol{\rho}; \boldsymbol{\lambda}) = C_2(\mathbf{s}) + \boldsymbol{\mu}^\top \mathbf{f}(\mathbf{s}) + \boldsymbol{\rho}^\top \mathbf{h}(\mathbf{s}; \boldsymbol{\lambda}),$$

where $\boldsymbol{\mu} \in \mathbb{R}^{2N}$ and $\boldsymbol{\rho} \geq \mathbf{0} \in \mathbb{R}^m$. Subsequently, the Karush-Kuhn-Tucker (KKT) [19], [20] optimality conditions are the set of nonlinear conditions that define a solution of (18):

$$\begin{aligned} \frac{\partial}{\partial \mathbf{s}} L(\mathbf{s}, \boldsymbol{\mu}, \boldsymbol{\rho}; \boldsymbol{\lambda}) &= \mathbf{0} \\ \mathbf{f}(\mathbf{s}) &= \mathbf{0} \\ \mathbf{h}(\mathbf{s}, \boldsymbol{\lambda}) &\geq \mathbf{0} \\ \boldsymbol{\rho}_i \mathbf{h}(\mathbf{s}, \boldsymbol{\lambda})_i &= 0, \quad i = 1, \dots, m \\ \boldsymbol{\rho} &\geq \mathbf{0}. \end{aligned} \quad (20)$$

The set of active inequality constraints is defined as

$$\mathcal{A}(\mathbf{s}) = \{i : \mathbf{h}(\mathbf{s}, \boldsymbol{\lambda})_i = 0\}.$$

Lagrange multipliers $\boldsymbol{\mu}, \boldsymbol{\rho}$ that satisfy the KKT conditions can be found when the columns of the constraint Jacobians are linearly independent, i.e., when

$$\left[\frac{\partial}{\partial \mathbf{s}} \mathbf{f}(\mathbf{s}), \quad \frac{\partial}{\partial \mathbf{s}} \mathbf{h}(\mathbf{s}, \boldsymbol{\lambda})_i \right], \quad i \in \mathcal{A}(\mathbf{s}), \quad (21)$$

are linearly independent. Moreover, second order conditions (which state that the Lagrangian Hessian is positive definite in the nullspace of the constraint derivatives) ensure strict

local optimality of a KKT point. Finally, if the active set is unchanged in a small neighborhood around $\boldsymbol{\lambda}$, then changes in \mathbf{s} with regards to changes in $\boldsymbol{\lambda}$ are continuous. Summarizing we assume the three conditions:

- 1) Linear independence in the constraint Jacobians (21)
- 2) Second order sufficient conditions hold for (18)
- 3) Strict complementary slackness: $\rho_i > 0, i \in \mathcal{A}(\mathbf{s})$.

The first two assumptions state that a local minimum for the problem in (18) exists. The third ensures continuity of derivatives, such as $\frac{\partial \mathbf{s}}{\partial \boldsymbol{\lambda}}$ and $\frac{\partial \boldsymbol{\lambda}_M}{\partial \boldsymbol{\lambda}}$. The analysis is reduced into three smaller parts using $(\boldsymbol{\lambda})_n = \lambda_n$ (the n^{th} element):

- Part I: Representation of $\frac{\partial \boldsymbol{\lambda}_M}{\partial \boldsymbol{\lambda}}$
- Part II: Sensitivities $\frac{\partial \mathbf{s}}{\partial \lambda_n}$ and $\frac{\partial^2 \mathbf{f}}{\partial \lambda_n \partial \mathbf{x}}$
- Part III: Bound on $\left\| \frac{\partial \boldsymbol{\lambda}_M}{\partial \boldsymbol{\lambda}} \right\|_2$ and Implications

A. Part I: Representation of $\frac{\partial \boldsymbol{\lambda}_M}{\partial \boldsymbol{\lambda}}$

This section develops the expressions that will be used later to deduce the condition for convergence. Thus the $\boldsymbol{\Gamma}$ matrix is represented as a function of \mathbf{s} and $\boldsymbol{\lambda}$: $\boldsymbol{\Gamma}(\mathbf{s}(\boldsymbol{\lambda})) = -\mathbf{J}(\mathbf{s}(\boldsymbol{\lambda}))^{-1}$, where $\mathbf{J}(\mathbf{s}(\boldsymbol{\lambda})) = \mathbf{J} = \partial \mathbf{f} / \partial \mathbf{x}$ (cf. (14)). For notation, we will be using the following definition

$$\mathbf{w}_r(\mathbf{s}(\boldsymbol{\lambda})) \equiv \boldsymbol{\Sigma} \boldsymbol{\Gamma}(\mathbf{s}(\boldsymbol{\lambda}))^\top \mathbf{e}_r, \quad (22)$$

and subsequently rewrite $(\boldsymbol{\lambda}_M(\mathbf{s}(\boldsymbol{\lambda})))_r = z_r [\mathbf{w}_r(\mathbf{s}(\boldsymbol{\lambda}))^\top \mathbf{w}_r(\mathbf{s}(\boldsymbol{\lambda}))]^{1/2}$. Because Condition 2 in (19) involves partial derivatives, we take the partial derivative with respect to λ_n (the ‘ n^{th} ’ tightening), so that $\frac{\partial}{\partial \lambda_n} (\boldsymbol{\lambda}_M(\mathbf{s}(\boldsymbol{\lambda})))_r = \frac{z_r^2}{\lambda_r} \left[\mathbf{w}_r^\top \frac{\partial \mathbf{w}_r}{\partial \lambda_n} \right]$, denoting $(\boldsymbol{\lambda}_M(\mathbf{s}(\boldsymbol{\lambda})))_r = \lambda_r$ in the right hand side. This expression provides a basis for what the matrix of partial derivatives will look like. For indices $1 \leq r \leq 2N$ and $1 \leq n \leq 2N$ the matrix of *sensitivities* with respect to the vector $\boldsymbol{\lambda}$ is

$$\frac{\partial \boldsymbol{\lambda}_M}{\partial \boldsymbol{\lambda}} = \begin{bmatrix} \frac{z_1^2}{\lambda_1} \left[\mathbf{w}_1^\top \frac{\partial \mathbf{w}_1}{\partial \lambda_1} \right] & \frac{z_1^2}{\lambda_1} \left[\mathbf{w}_1^\top \frac{\partial \mathbf{w}_1}{\partial \lambda_2} \right] & \dots & \frac{z_1^2}{\lambda_1} \left[\mathbf{w}_1^\top \frac{\partial \mathbf{w}_1}{\partial \lambda_n} \right] \\ \frac{z_2^2}{\lambda_2} \left[\mathbf{w}_2^\top \frac{\partial \mathbf{w}_2}{\partial \lambda_1} \right] & \frac{z_2^2}{\lambda_2} \left[\mathbf{w}_2^\top \frac{\partial \mathbf{w}_2}{\partial \lambda_2} \right] & \dots & \frac{z_2^2}{\lambda_2} \left[\mathbf{w}_2^\top \frac{\partial \mathbf{w}_2}{\partial \lambda_n} \right] \\ \vdots & \vdots & \ddots & \vdots \\ \frac{z_r^2}{\lambda_r} \left[\mathbf{w}_r^\top \frac{\partial \mathbf{w}_r}{\partial \lambda_1} \right] & \frac{z_r^2}{\lambda_r} \left[\mathbf{w}_r^\top \frac{\partial \mathbf{w}_r}{\partial \lambda_2} \right] & \dots & \frac{z_r^2}{\lambda_r} \left[\mathbf{w}_r^\top \frac{\partial \mathbf{w}_r}{\partial \lambda_n} \right] \end{bmatrix} \quad (23)$$

Note that since \mathbf{w}_r^\top is a row vector and $\frac{\partial \mathbf{w}_r}{\partial \lambda_n}$ is a column vector the entries in (23) can be written as

$$\mathbf{w}_r^\top \frac{\partial \mathbf{w}_r}{\partial \lambda_n} = \|\mathbf{w}_r\|_2 \left\| \frac{\partial \mathbf{w}_r}{\partial \lambda_n} \right\|_2 \cos(\phi_{rn}), \quad (24)$$

where ϕ_{rn} represents the angle between \mathbf{w}_r and $\frac{\partial \mathbf{w}_r}{\partial \lambda_n}$. Since $\lambda_r = z_r \|\mathbf{w}_r\|_2$ and $\|\mathbf{w}_r\|_2 = \frac{\lambda_r}{z_r}$, therefore the elements of the matrix in (23) are $\frac{z_r^2}{\lambda_r} \left[\mathbf{w}_r^\top \frac{\partial \mathbf{w}_r}{\partial \lambda_n} \right] = z_r \left\| \frac{\partial \mathbf{w}_r}{\partial \lambda_n} \right\|_2 \cos(\phi_{rn})$. From (22) it holds that $\left\| \frac{\partial \mathbf{w}_r}{\partial \lambda_n} \right\|_2 = \left\| \boldsymbol{\Sigma} \frac{\partial \boldsymbol{\Gamma}^\top}{\partial \lambda_n} \mathbf{e}_r \right\|_2$, which yields the subsequent inequalities

$$\left(\frac{\partial \boldsymbol{\lambda}_M}{\partial \boldsymbol{\lambda}} \right)_{rn} \leq |z_r| \|\boldsymbol{\Sigma}\|_2 \left\| \frac{\partial \boldsymbol{\Gamma}^\top}{\partial \lambda_n} \mathbf{e}_r \right\|_2. \quad (25)$$

Note that z_r and $\boldsymbol{\Sigma}$ are constants, with upper bounds $z_r \leq \max_{1 \leq r \leq 2N} |z_r| \equiv K_1$ and $\|\boldsymbol{\Sigma}\|_2 \leq K_2$. Therefore, a bound for $\left\| \frac{\partial \boldsymbol{\Gamma}^\top}{\partial \lambda_n} \mathbf{e}_r \right\|_2$ fully specifies (25), and thus the elements of (23).

B. Part II: Sensitivities $\frac{\partial \mathbf{s}}{\partial \lambda_n}$ and $\frac{\partial^2 \mathbf{f}}{\partial \lambda_n \partial \mathbf{x}}$

In order to derive a bound on $\left\| \frac{\partial \boldsymbol{\Gamma}^\top}{\partial \lambda_n} \mathbf{e}_r \right\|_2 = \|\mathbf{e}_r^\top \frac{\partial \boldsymbol{\Gamma}}{\partial \lambda_n}\|_2$, recall that $\boldsymbol{\Gamma}(\mathbf{s}(\boldsymbol{\lambda})) = \mathbf{J}(\mathbf{s}(\boldsymbol{\lambda}))^{-1} = \mathbf{J}^{-1}$. In this respect, note that we can make use of the identity

$$\frac{\partial}{\partial \lambda_n} \mathbf{J}^{-1} = -\mathbf{J}^{-1} \left(\frac{\partial}{\partial \lambda_n} \mathbf{J} \right) \mathbf{J}^{-1}.$$

Specifically, defining the vector $\mathbf{j}_r^\top \equiv \mathbf{e}_r^\top \mathbf{J}^{-1}$ then

$$\left\| \mathbf{e}_r^\top \frac{\partial \mathbf{J}^{-1}}{\partial \lambda_n} \right\|_2 = \left\| \mathbf{j}_r^\top \frac{\partial \mathbf{J}}{\partial \lambda_n} \mathbf{J}^{-1} \right\|_2 \leq \|\mathbf{J}^{-1}\|_2 \left\| \mathbf{j}_r^\top \frac{\partial \mathbf{J}}{\partial \lambda_n} \right\|_2.$$

With a bound on $\|\mathbf{J}(\mathbf{s}(\boldsymbol{\lambda}))^{-1}\|_2 \leq K_\Gamma$ (from (16)), it remains to derive an upper bound on $\left\| \mathbf{j}_r^\top \frac{\partial}{\partial \lambda_n} \mathbf{J}(\mathbf{s}(\boldsymbol{\lambda})) \right\|_2$. Next we describe the essential components for such a bound, based on the elements of the 2nd derivative matrices

$$\frac{\partial}{\partial \lambda_n} \mathbf{J}(\mathbf{s}(\boldsymbol{\lambda})) = \frac{\partial}{\partial \lambda_n} \left(\frac{\partial \mathbf{f}}{\partial \mathbf{x}} \right) = \begin{bmatrix} \frac{\partial^2 \mathbf{f}}{\partial \lambda_n \partial \mathbf{q}_G^g} & \frac{\partial^2 \mathbf{f}}{\partial \lambda_n \partial \mathbf{v}_L} & \frac{\partial^2 \mathbf{f}}{\partial \lambda_n \partial \boldsymbol{\theta}} \end{bmatrix}.$$

The elements of $\frac{\partial}{\partial \lambda_n} \left(\frac{\partial \mathbf{f}}{\partial \mathbf{x}} \right)$ can be computed from (15) once

$$\frac{\partial}{\partial \lambda_n} v_i \equiv \partial_n v_i, \quad \frac{\partial}{\partial \lambda_n} \theta_i \equiv \partial_n \theta_i, \quad (26)$$

for $1 \leq n \leq 2N$, $1 \leq i \leq N$ are known. This is the case, because $\frac{\partial}{\partial \lambda_n} (v_i c_{ki})$ and $\frac{\partial}{\partial \lambda_n} (v_i d_{ki})$, for $1 \leq k \leq N$, (in e.g., (15)) can be computed from these quantities. In classical nonlinear programming theory, using the assumptions in Section III, the existence of a parametrized solution to (18) with dependence on $\boldsymbol{\lambda}$ is defined by

$$\mathbf{a}(\boldsymbol{\lambda}) \equiv \begin{bmatrix} \mathbf{s}(\boldsymbol{\lambda}) \\ \boldsymbol{\mu}(\boldsymbol{\lambda}) \\ \boldsymbol{\rho}(\boldsymbol{\lambda}) \end{bmatrix}.$$

Selecting a set of rows in $\mathbf{a}(\boldsymbol{\lambda})$, extracts $\mathbf{s}(\boldsymbol{\lambda})$. The derivative of $\mathbf{a}(\boldsymbol{\lambda})$ w.r.t. $\boldsymbol{\lambda}$ can be computed from the KKT conditions

$$\begin{bmatrix} \frac{\partial}{\partial \mathbf{s}} L(\mathbf{a}(\boldsymbol{\lambda}), \boldsymbol{\lambda}) \\ \mathbf{f}(\mathbf{s}(\boldsymbol{\lambda})) \\ \boldsymbol{\rho}_i \mathbf{h}(\mathbf{s}(\boldsymbol{\lambda}), \lambda)_i \end{bmatrix} \equiv \mathbf{G}(\mathbf{a}(\boldsymbol{\lambda}), \boldsymbol{\lambda}) = \mathbf{0}, \quad i \in \mathcal{A}(\mathbf{s}). \quad (27)$$

From (27) it holds that

$$\frac{\partial}{\partial \lambda_n} \mathbf{G}(\mathbf{a}(\boldsymbol{\lambda}), \boldsymbol{\lambda}) = \frac{\partial \mathbf{G}}{\partial \mathbf{a}} \frac{\partial \mathbf{a}}{\partial \lambda_n} + \frac{\partial \mathbf{G}}{\partial \boldsymbol{\lambda}_n} = \mathbf{0},$$

and $\frac{\partial \mathbf{a}}{\partial \lambda_n} = -\left[\frac{\partial \mathbf{G}}{\partial \mathbf{a}} \right]^{-1} \frac{\partial \mathbf{G}}{\partial \lambda_n}$. Thus $\frac{\partial \mathbf{s}}{\partial \lambda_n}$ is obtained by extracting elements from $\frac{\partial \mathbf{a}}{\partial \lambda_n}$. The existence of the inverse and hence the derivatives of \mathbf{a} are guaranteed by [16, Theorem 3.2]. Because the derivatives are finite a bound of the form $\left\| \frac{\partial \mathbf{a}}{\partial \lambda_n} \right\|_2 \leq K_a$ exists, which implies $\left\| \frac{\partial \mathbf{s}}{\partial \lambda_n} \right\|_2 \leq K_a$ and $\left\| \frac{\partial \mathbf{x}}{\partial \lambda_n} \right\|_2 \leq K_a$.

Moreover, the partial derivatives of $\frac{\partial}{\partial \lambda_n} \left(\frac{\partial \mathbf{f}}{\partial \mathbf{x}} \right)$ are computed from (15) from which $\frac{\partial}{\partial \lambda_n} \left(\frac{\partial \mathbf{f}}{\partial \mathbf{q}_G^g} \right) = \mathbf{0}$. Since the power flow equations hold with equality at the solution, we simplify the summations in (15), using the definitions $p_i^{\text{net}} \equiv p_i^g - p_i^d$, $q_i^{\text{net}} \equiv q_i^g - q_i^d$, as e.g., $\sum_{k=1}^N v_k c_{ik} = \frac{p_i^{\text{net}}}{v_i}$ (and correspondingly for

the other terms). Then for $1 \leq i \leq N$ and $j = N + i$ as well as $1 \leq l \leq N_L$ and $1 \leq t \leq N$

$$\begin{aligned} \frac{\partial}{\partial \lambda_n} \left(\frac{\partial \mathbf{f}}{\partial \mathbf{v}_L} \right)_{i,l} &= \begin{cases} \partial_n \left(\frac{p_i^{\text{net}}}{v_i} \right) + 2\partial_n(c_{ii}v_i) & \text{if } i = [L]_l \\ \partial_n(v_i c_{i[l]_l}) & \text{otherwise} \end{cases} \\ \frac{\partial}{\partial \lambda_n} \left(\frac{\partial \mathbf{f}}{\partial \mathbf{v}_L} \right)_{j,l} &= \begin{cases} \partial_n \left(\frac{q_i^{\text{net}}}{v_i} \right) + 2\partial_n(d_{ii}v_i) & \text{if } i = [L]_l \\ \partial_n(v_i d_{i[l]_l}) & \text{otherwise} \end{cases} \\ \frac{\partial}{\partial \lambda_n} \left(\frac{\partial \mathbf{f}}{\partial \boldsymbol{\theta}} \right)_{i,t} &= \begin{cases} -\partial_n q_i^{\text{net}} & \text{if } i = t \\ v_k d_{ik} \partial_n v_i + v_i \partial_n(v_k d_{ik}) & \text{otherwise} \end{cases} \\ \frac{\partial}{\partial \lambda_n} \left(\frac{\partial \mathbf{f}}{\partial \boldsymbol{\theta}} \right)_{j,t} &= \begin{cases} \partial_n q_i^{\text{net}} & \text{if } i = t \\ -(v_k c_{ik} \partial_n v_i + v_i \partial_n(v_k c_{ik})) & \text{otherwise} \end{cases} \end{aligned}$$

These derivatives can be bounded with limits on $\partial_n p_i^{\text{net}}, \partial_n q_i^{\text{net}}, \partial_n v_i, \partial_n \theta_i, \partial_n c_{ik}, \partial_n d_{ik}, \partial_n(v_k c_{ik})$, and $\partial_n(v_k d_{ik})$ (i.e., all elements that appear in the expression of the derivatives). Since all these individual elements are bounded by K_a , and since the c_{ik}, d_{ik} terms are bounded, too (they depend on v_i, θ_i), the maximum element will be bounded by a constant, as well. Denote this constant by K_x , then

$$\max_{1 \leq i, j \leq 2N} \left| \left(\frac{\partial}{\partial \lambda_n} \left(\frac{\partial \mathbf{f}}{\partial \mathbf{x}} \right) \right)_{ij} \right| \equiv K_x.$$

With this, since $\|\mathbf{j}_r\|_2 \leq K_\Gamma$ and $\frac{\partial^2 \mathbf{f}}{\partial \lambda_n \partial \mathbf{x}} = \frac{\partial}{\partial \lambda_n} \mathbf{J}(\mathbf{s}(\boldsymbol{\lambda}))$, we obtain the upper bound

$$\left\| \mathbf{j}_r^\top \frac{\partial \mathbf{J}(\mathbf{s}(\boldsymbol{\lambda}))}{\partial \lambda_n} \right\|_2 \leq 2K_\Gamma K_x N. \quad (28)$$

C. Part III: Bound on $\left\| \frac{\partial \boldsymbol{\lambda}_M}{\partial \boldsymbol{\lambda}} \right\|_2$ and Implications

The analysis from the previous section has implications for the convergence of Algorithm 1. In particular, since $\|\mathbf{J}(\mathbf{s}(\boldsymbol{\lambda}))^{-1}\|_2 \leq K_\Gamma$ (cf. Section I-C2) a bound on the magnitude of (23) can be found. By combining (25) and (28) and noting that typically only $N_A \ll 4N + N_L$ inequality constraints are active at the solution, the upper bound is

$$\left\| \frac{\partial \boldsymbol{\lambda}_M}{\partial \boldsymbol{\lambda}} \right\|_2 \leq 2 \cdot \|\boldsymbol{\Sigma}\|_2 \cdot K_1 \cdot K_\Gamma \cdot K_x \cdot N_A \cdot N. \quad (29)$$

If the right hand side in (29) is less than one then Condition 2 in (19) of the fixed point iteration is guaranteed to hold. The upper bound in (29) is composed of the parts

$$\|\boldsymbol{\Sigma}\|_2, \quad K_1, \quad K_\Gamma \cdot K_x \cdot N_A \cdot N.$$

Typically, there is digression on the values of K_1 and $\|\boldsymbol{\Sigma}\|_2$, whereas $K_\Gamma \cdot K_x \cdot N_A \cdot N$ is problem (network specification) dependent. For instance, K_1 is reduced by reducing the probability constraints in (6). Concretely, if all $\epsilon \rightarrow 1/2$ then $K_1 \rightarrow 0$. Secondly, $\|\boldsymbol{\Sigma}\|_2$ is regarded as a parameter to the iterative algorithm and lower values of this parameter promote faster convergence. *In particular, if $\|\boldsymbol{\Sigma}\|_2$ is small enough (sufficiently small uncertainty) then from (19) the fixed point iteration is guaranteed to converge.* Finally, the bound (29) includes the network dimension N . In numerical experiments, we observe that setting $\|\boldsymbol{\Sigma}\|_2 \sim \mathcal{O}(1/N^2)$ enables the solution of large networks.

D. Computing a Bound Estimate

Before applying Algorithm 1 for multiple iterations the bound in (29) can be qualitatively used to assess the convergence behavior of the method. In particular, at $k = 0$, use $\mathbf{s}^{(1)}$ to compute the right hand side in (29). Computing K_Γ is available from a LU factorization of \mathbf{J} . The computation of K_x can be approximated by first estimating K_a from a lower bound on the smallest singular value of $\partial \mathbf{G} / \partial \mathbf{a}$ using [15] (as for (16)), calling such an estimate \hat{K}_a . Because $\boldsymbol{\lambda}$ appears linearly in the inequalities $\mathbf{h}(\mathbf{s}, \boldsymbol{\lambda}) = \text{vec}(\mathbf{g}_1(\mathbf{s}), \mathbf{g}_2(\mathbf{s}) + \boldsymbol{\lambda})$ (for appropriately defined $\mathbf{g}_1(\mathbf{s}), \mathbf{g}_2(\mathbf{s})$) and in no other constraints, the expression $\partial \mathbf{G} / \partial \lambda_n = \text{vec}(\mathbf{0}, \mathbf{e}_n)$ simplifies. Subsequently, $K_a \sim 1/\hat{K}_a$ and $K_x = aK_a$, for a constant $a > 0$. If the computed bound, say $B^{(0)}$ exceeds a fixed threshold, set $\boldsymbol{\Sigma}^{\text{Scaled}} = 1/B^{(0)} \boldsymbol{\Sigma}$. This ensures that $\|\partial \lambda_r / \partial \boldsymbol{\lambda}\|_2 \leq \|\boldsymbol{\Sigma}\|_2$ in subsequent iterations. Moreover, we include a scaling factor γ_g in computing the line flow constraint tightenings from (13), thus $\bar{\lambda}_{r_1} = \gamma_g \lambda_{r_1}$. Note that for $\gamma_g = 1$ no scaling is included.

IV. NUMERICAL EXPERIMENTS

This section describes numerical experiments on a set of standard IEEE test problems. Typically, solving large chance-constrained optimization problems is numerically very challenging. Even directly solving the reformulated problem in (17) with state-of-the-art general purpose methods becomes quickly intractable. Therefore, for larger networks we apply Algorithm 1 to approximately solve (17). Our implementation of Algorithm 1 uses Julia 1.1.0 [21] and the modeling libraries JuMP v0.18.6 [22] and StructJuMP [23]. In particular, in order to solve the AC-OPF problem from (2) and its modifications in Line 3 of Algorithm 1 we use the general purpose nonlinear optimization solver IPOPT [24]. The stopping criteria in Algorithm 1 are set as $\tau_q = 1 \times 10^{-3}$, $\tau_v = 1 \times 10^{-5}$, $\tau_\theta = 1 \times 10^{-5}$, $\tau_g = 1 \times 10^{-3}$. Unless otherwise stated, we set $\boldsymbol{\Sigma} = \sigma \mathbf{I}$, $\sigma = 1/N^2$ and $\boldsymbol{\epsilon} = \text{vec}(\epsilon_q, \epsilon_v, \epsilon_\theta, \epsilon_g) = \text{vec}(0.1, 0.1, 0.1, 0.2)$, and $\gamma_g = 1/N_L^2$. The initial values are computed as the midpoint between the upper and lower bounds $\mathbf{s}^{(0)} = 1/2(\mathbf{u} + \mathbf{l})$. The maximum number of iterations for Algorithm 1 is set as $\text{maxiter} = 50$. The test cases are summarized in Table I: The

TABLE I
TEST CASES. COLUMN 2 CONTAINS THE TOTAL NUMBER OF NODES IN THE NETWORK, N , AND THEIR SPLIT AMONG GENERATORS, N_G , AND LOADS, N_L . THE LARGEST CASE CONTAINS MORE THAN $9000 < N$ NODES.

| Problem | $N = N_G + N_L$ | N_{line} | Reference |
|-----------------|----------------------|-------------------|-----------|
| IEEE 9 | $9 = 3 + 6$ | 9 | [6] |
| IEEE 30 | $30 = 6 + 24$ | 41 | [6], [25] |
| IEEE 118 | $118 = 54 + 64$ | 186 | [6] |
| IEEE 300 | $300 = 69 + 231$ | 411 | [6] |
| IEEE 1354pegase | $1354 = 260 + 1094$ | 1991 | [26] |
| IEEE 2869pegase | $2869 = 510 + 2359$ | 4582 | [26] |
| IEEE 9241pegase | $9241 = 1445 + 7796$ | 16049 | [26] |

numerical experiments are divided into two parts. Experiment I compares solutions to (17) using a direct solver (i.e., IPOPT) or the iterative approach from Algorithm 1. Experiment II reports convergence results on the test problems from Table I.

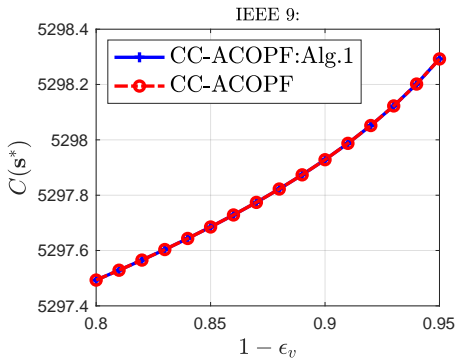


Fig. 1. Comparison of optimal objective function values using CC-ACOPF (direct approach) and CC-ACOPF:Alg.1. The optimal objective function values nearly coincide on this IEEE 9 bus case as the parameters ϵ_v (probability thresholds) vary.

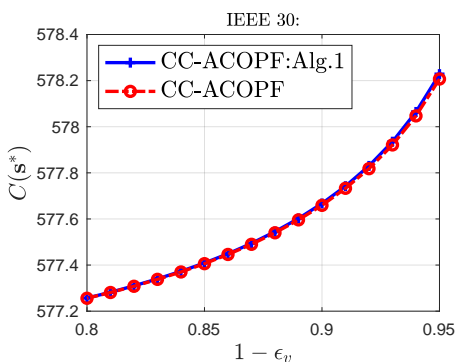


Fig. 2. Comparison of optimal objective function values using CC-ACOPF (direct approach) and CC-ACOPF:Alg.1. Also on this IEEE 30 bus case the optimal objective function values nearly coincide as the parameters ϵ_v (probability thresholds) vary.

A. Experiment I

This experiment compares the optimal objective function values of solving (17) directly (CC-ACOPF) using IPOPT or using Algorithm 1 (CC-ACOPF:Alg.1). Solving (17) in JuMP becomes computationally intractable beyond $N = 100$, because the inverse, $\Gamma(\mathbf{s}) \in \mathbb{R}^{2N \times 2N}$, and its derivatives are continuously recomputed. For this reason, we compare CC-ACOPF and CC-ACOPF:Alg.1 for the 9 bus and 30 bus cases (which are both tractable by the direct approach). In particular, we compare the solved objective function values after perturbing the problem formulation slightly. Specifically, we compare the computed objective function values when the values $\epsilon_v = \{0.05, 0.06, \dots, 0.2\}$ change the probability constraints. (Varying other parameters yields similar results). The outcomes of the 9 bus network are in Figure 1. Figure 2 contains the outcomes of applying both approaches on the 30 bus network. Observe in both figures that the optimal objective function values, i.e., $C(\mathbf{s}^*)$, increase as the values of $1 - \epsilon_v$ increase. This is because larger values of $1 - \epsilon_v$ correspond to stricter chance constraints. Importantly, observe that the objective function values are virtually equivalent for these test cases, as the values of the blue and red curves nearly exactly match up. However, the main advantage of Algorithm 1 is that it scales to larger cases, too.

TABLE II
COMPARISON OF ALGORITHM 1 (CC-ACOPF:ALG.1) AND A DIRECT SOLUTION APPROACH (CC-ACOPF) ON A SET OF IEEE POWER FLOW NETWORKS. THE LAST 6 ROWS IN THE “OBJECTIVE” COLUMN FOR CC-ACOPF ARE LABELED N/A, BECAUSE THIS APPROACH TOOK COMPUTATIONAL TIMES IN EXCESS OF 5 HOURS.

| IEEE | CC-ACOPF:Alg.1 | | | CC-ACOPF | |
|------|----------------|-----------|-----------|------------------|-----------|
| | Its. | Objective | Time(sec) | Objective | Time(sec) |
| 9 | 4 | 5297.928 | 0.0504 | 5297.928 | 0.3075 |
| 30 | 4 | 578.0081 | 0.2216 | 577.9815 | 217.10 |
| 118 | 3 | 129662.0 | 0.4710 | N/A [†] | >5h |
| 300 | 5 | 720090.3 | 4.3123 | N/A [†] | >5h |
| 1354 | 3 | 74069.38 | 75.039 | N/A [†] | >5h |
| 2383 | 3 | 1868551. | 236.27 | N/A [†] | >5h |
| 2869 | 3 | 133999.3 | 316.80 | N/A [†] | >5h |
| 9241 | 3 | 315912.6 | 3255.2 | N/A [†] | >5h |

B. Experiment II

Experiment II reports results of applying Algorithm 1 (CC-ACOPF:Alg.1) and a direct solver (CC-ACOPF) to the problem from (17) on the test problems in table IV. For CC-ACOPF:Alg.1 the number of iterations, time and “optimal” objective values are reported. For CC-ACOPF the “optimal” objective values and the time are reported. Algorithm 1 converged on all of the reported problems. These problems include large network instances, too. Observe in Table IV-B that for problems on which both solvers can be used, the optimal objective function values are close to each other. However, for large problems only Algorithm 1, based on a fixed point iteration, is practical.

V. CONCLUSION

This article develops a chance constrained AC optimal power flow model, in which the objective function only depends on deterministic variables and therefore enables immediate interpretation of the optimal function values. By linearizing the stochastic variables, a deterministic nonlinear optimization problem is described in lieu of the probabilistic one. Because solving the reformulated optimization problem is computationally challenging, we analyze the convergence criteria for a fixed point algorithm that solves a sequence of modified AC optimal power flow problems and enables scaling to larger network sizes. The analysis connects the model’s variance of the uncertainty and the constraint probabilities to the convergence properties of the algorithm. In numerical experiments, we compare the fixed point iteration to directly solving the reformulated problem and test the method on IEEE problems, including a network with over 9000 nodes. Certainly our bounds are quite conservative in this version. However, this the first attempt at proving convergence of the approach. Since iteratively resolving a sequence of tractable optimization problems (by holding specific nonlinear terms fixed) has been very effective on a variety of power systems applications, our analysis of such a fixed point method lays the ground for the convergence criteria of new future algorithms in this category.

ACKNOWLEDGEMENTS

This work was supported by the U.S. Department of Energy, Office of Science, Advanced Scientific Computing Research,

under Contract DE-AC02-06CH11357 at Argonne National Laboratory and by NSF through award CNS-51545046. We acknowledge fruitful discussion with Dr. Line Roald, who pointed out that Algorithm 1 was observed to cycle between different points, and encouraged an analysis of its convergence criteria. We also thank Eric Grimm, who helped in carrying out parts of the numerical experiments in Section IV.

REFERENCES

- [1] H. Zhang and P. Li, "Chance constrained programming for optimal power flow under uncertainty," *IEEE Transactions on Power Systems*, vol. 26, no. 4, pp. 2417–2424, Nov 2011.
- [2] G. Li and X. P. Zhang, "Stochastic optimal power flow approach considering correlated probabilistic load and wind farm generation," in *IET Conference on Reliability of Transmission and Distribution Networks (RTDN 2011)*, Nov 2011, pp. 1–7.
- [3] M. Hojjat and M. H. Javidi, "Chance-constrained programming approach to stochastic congestion management considering system uncertainties," *IET Generation, Transmission Distribution*, vol. 9, no. 12, pp. 1421–1429, 2015.
- [4] K. Baker, E. Dall’Anese, and T. Summers, "Distribution-agnostic stochastic optimal power flow for distribution grids," in *2016 North American Power Symposium (NAPS)*, Sep. 2016, pp. 1–6.
- [5] M. Vrakopoulou, M. Katsampani, K. Margellos, J. Lygeros, and G. Andersson, "Probabilistic security-constrained ac optimal power flow," in *2013 IEEE Grenoble Conference*, June 2013, pp. 1–6.
- [6] R. D. Zimmerman, C. E. Murillo-Sánchez, and R. J. Thomas, "Matpower: Steady-state operations, planning, and analysis tools for power systems research and education," *IEEE Transactions on Power Systems*, vol. 26, no. 1, pp. 12–19, Feb 2011.
- [7] M. Lubin, Y. Dvorkin, and L. Roald, "Chance constraints for improving the security of ac optimal power flow," *IEEE Transactions on Power Systems*, vol. 34, no. 3, pp. 1908–1917, 2019.
- [8] D. Bienstock, M. Chertkov, and S. Harnett, "Chance-constrained optimal power flow: Risk-aware network control under uncertainty," *SIAM Review*, vol. 56, no. 3, pp. 461–495, 2014.
- [9] D. Lee, K. Turitsyn, D. K. Molzahn, and L. A. Roald, "Feasible path identification in optimal power flow with sequential convex restriction," *IEEE Transactions on Power Systems*, vol. 35, no. 5, pp. 3648–3659, 2020.
- [10] V. Frolov, L. Roald, and M. Chertkov, "Cloud-ac-opf: Model reduction technique for multi-scenario optimal power flow via chance-constrained optimization," in *2019 IEEE Milan PowerTech*, 2019, pp. 1–6.
- [11] L. Roald and G. Andersson, "Chance-constrained ac optimal power flow: Reformulations and efficient algorithms," *IEEE Transactions on Power Systems*, vol. 33, no. 3, pp. 2906–2918, May 2018.
- [12] J. Schmidli, L. Roald, S. Chatzivasileiadis, and G. Andersson, "Stochastic ac optimal power flow with approximate chance-constraints," in *2016 IEEE Power and Energy Society General Meeting (PESGM)*, July 2016, pp. 1–5.
- [13] R. G. J. Miller, *Simultaneous Statistical Inference*. Springer-Verlag New York, 1981.
- [14] D. Bienstock, *Electrical Transmission System Cascades and Vulnerability*. Philadelphia, PA: Society for Industrial and Applied Mathematics, 2015. [Online]. Available: <https://epubs.siam.org/doi/abs/10.1137/1.9781611974164>
- [15] Y. Hong and C.-T. Pan, "A lower bound for the smallest singular value," *Linear Algebra and its Applications*, vol. 172, pp. 27 – 32, 1992. [Online]. Available: <http://www.sciencedirect.com/science/article/pii/0024379592900164>
- [16] A. V. Fiacco and J. Kyparisis, "Sensitivity analysis in nonlinear programming under second order assumptions," in *Systems and Optimization*, A. Bagchi and H. T. Jongen, Eds. Berlin, Heidelberg: Springer Berlin Heidelberg, 1985, pp. 74–97.
- [17] A. V. Fiacco, "Nonlinear programming sensitivity analysis results using strong second order assumptions," in *Numerical Optimization of Dynamic Systems*, L. C. W. Dixon and e. G. P. Szegő, Eds. North-Holland, Amsterdam: Springer Berlin Heidelberg, 1980, pp. 327–348.
- [18] S. H. Strogatz, *Nonlinear Dynamics and Chaos: With Applications to Physics, Biology, Chemistry, and Engineering*. Addison-Wesley, 1994.
- [19] W. Karush, "Minima of functions of several variables with inequalities as side conditions," Master’s thesis, Department of Mathematics, University of Chicago, Illinois, USA, 1939.
- [20] H. W. Kuhn and A. W. Tucker, "Nonlinear programming," in *Proceedings of the Second Berkeley Symposium on Mathematical Statistics and Probability*. Berkeley, Calif.: University of California Press, 1951, pp. 481–492. [Online]. Available: <https://projecteuclid.org/euclid.bsm/1200500249>
- [21] J. Bezanson, A. Edelman, S. Karpinski, and V. B. Shah, "Julia: A fresh approach to numerical computing," *SIAM review*, vol. 59, no. 1, pp. 65–98, 2017. [Online]. Available: <https://doi.org/10.1137/141000671>
- [22] I. Dunning, J. Huchette, and M. Lubin, "Jump: A modeling language for mathematical optimization," *SIAM Review*, vol. 59, no. 2, pp. 295–320, 2017.
- [23] M. Anitescu and G. C. Petra, "StructJuMP a block-structured optimization framework for jump," <https://github.com/StructJuMP/StructJuMP.jl> (retrieved Mar. 27th, 2019), 2019.
- [24] A. Wächter and L. T. Biegler, "On the implementation of an interior-point filter line-search algorithm for large-scale nonlinear programming," *Math. Program.*, vol. 106, pp. 25–57, 2006.
- [25] O. Alsac and B. Stott, "Optimal load flow with steady-state security," *IEEE Transactions on Power Apparatus and Systems*, vol. PAS-93, no. 3, pp. 745–751, May 1974.
- [26] S. Fliscounakis, P. Panciatici, F. Capitanescu, and L. Wehenkel, "Contingency ranking with respect to overloads in very large power systems taking into account uncertainty, preventive, and corrective actions," *IEEE Transactions on Power Systems*, vol. 28, no. 4, pp. 4909–4917, Nov 2013.



Johannes Brust is a postdoctoral researcher in the in the Mathematics and Computer Science Division at Argonne National Laboratory, IL. He received a M.Sc. in financial engineering from Maastricht University and a Ph.D. in applied mathematics from the University of California, Merced. His research is on effective large scale computational methods applied to optimal power flow problems.



Mihai Anitescu Is a senior computational mathematician in the Mathematics and Computer Science Division at Argonne National Laboratory and a professor in the Department of Statistics at the University of Chicago. He obtained his engineer diploma (electrical engineering) from the Polytechnic University of Bucharest in 1992 and his Ph.D. in applied mathematical and computational sciences from the University of Iowa in 1997. He specializes in the areas of numerical optimization, computational science, numerical analysis and uncertainty

quantification in which he has published more than 100 papers in scholarly journals and book chapters. He is on the editorial board of the SIAM Journal on Optimization and he is a senior editor for Optimization Methods and Software, he is a past member of the editorial boards of the Mathematical Programming A and B, SIAM Journal on Uncertainty Quantification, and SIAM Journal on Scientific Computing. He has been recognized for his work in applied mathematics by his selection as a SIAM Fellow in 2019.

The submitted manuscript has been created by UChicago Argonne, LLC, Operator of Argonne National Laboratory ("Argonne"). Argonne, a U.S. Department of Energy Office of Science laboratory, is operated under Contract No. DE-AC02-06CH11357. The U.S. Government retains for itself, and others acting on its behalf, a paid-up nonexclusive, irrevocable worldwide license in said article to reproduce, prepare derivative works, distribute copies to the public, and perform publicly and display publicly, by or on behalf of the Government. The Department of Energy will provide public access to these results of federally sponsored research in accordance with the DOE Public Access Plan. <http://energy.gov/downloads/doe-public-accessplan>